Hindawi
Mathematical Problems in Engineering
Volume 2022, Article ID 7666571, 13 pages
https://doi.org/10.1155/2022/7666571

Research Article

New Series Approach Implementation for Solving Fuzzy Fractional Two-Point Boundary Value Problems Applications

Dulfikar Jawad Hashim,[1] N. R. Anakira,[2] Ali Fareed Jameel,[3,4] A. K. Alomari,[5] Hamzeh Zureigat,[6] M. W. Alomari ,[2] and Teh Yuan Ying[4]

[1]*National University of Science and Technology, Dhi Qar, Nasiriyah, Iraq*
[2]*Department of Mathematics, Faculty of Science and Technology, Irbid National University, Irbid 2600, Jordan*
[3]*Faculty of Education and Arts, Sohar University, Sohar 3111, Oman*
[4]*Institute of Strategic Industrial Decision Modelling (ISIDM), School of Quantitative Sciences (SQS), Universiti Utara Malaysia (UUM), Kedah, Sintok 06010, Malaysia*
[5]*Department of Mathematics, Faculty of Science, Yarmouk University, Irbid 211-63, Jordan*
[6]*Departments of Mathematics, Faculty of Science and Technology, Jadara University, Irbid 21110, Jordan*

Correspondence should be addressed to M. W. Alomari; alomari@inu.edu.jo

Received 13 May 2022; Accepted 20 September 2022; Published 20 October 2022

Academic Editor: Cenap Özel

In this work, the fuzzy fractional two-point boundary value problems (FFTBVPs) are analyzed and solved using the fuzzy fractional homotopy analysis method (FF-HAM). Fuzzy set theory mixed with Caputo fractional derivative properties is utilized to produce a new formulation of the standard HAM in the fuzzy domain for the persistence of approximation series solutions for fuzzy fractional differential equations with boundary conditions. The FF-HAM provides a suitable way of controlling the convergence of the series solution through the advantage of the convergence control parameter, which plays a pivotal role in solving a wide range of mathematical problems. The convergence analysis algorithm has been described, along with a graphical representation of the FF-HAM of the proposed applications. The method produces high accuracy solutions with simple implementation for solving linear and nonlinear fuzzy fractional boundary value problems associated with physical application. Also, the obtained results are analyzed and compared with those present in the literature to show the efficiency of the FF-HAM.

1. Introduction

Fractional problems involving ordinary differential equations (FDEs) have received much interest recently as they are adequate models for certain physical phenomena [1]. Many important phenomena in electromagnetics, acoustics, viscoelasticity, electrochemistry, and material science are well described under fractional derivatives in the sense of fractional numbers [2–7]. It is well known that the fractional-order differential operators are nonlocal operators. This is one reason why fractional differential operators provide an excellent instrument for describing memory and hereditary properties of various physical processes [8]. But it always faces some obstacles besides complexity, namely, uncertainty and imprecision [9]. One of several advantages of employing the theory of fuzzy sets around fractional calculus theory is to develop formulation methodology and solve these complex problems that are accompanied by a lack of data, measurement errors, or when supplementary conditions are determined to be acceptable for analysis [10]. Such problems are too complicated or undefined for traditional methods. Therefore, fuzziness may also be a form of inaccuracy arising from the grouping of objects into groups that do not have clearly defined borders, so fuzzy set theory helps to handle these problems [11] by making fuzzy fractional ordinary differential equations (FFDEs) a reliable alternative to FDEs. Therefore, a mathematical model for many dynamical real-life problems can be represented by a system of ordinary differential equations. To model a dynamic system based on the long memory term that is inadequate of its behavior and has uncertain nature, FFDEs are a useful tool to be considered.

A boundary value problem is a differential equation with additional constraints called boundary conditions. A solution to a boundary value problem is a solution to the differential equation that also satisfies the boundary conditions. The second order fuzzy fractional differential equations have recently attracted the attention of many researchers to their considerable importance in science, especially after defining the fuzzy Caputo's Hukuhara derivative of order $1 < \rho \leq 2$ [12]. Even though these equations play a vital role in describing the most complex physical phenomena, they remain unimportant until they are solved. On the other hand, most lack accurate analytical solutions, so researchers have resorted to developing new methods that help engineers and physicists find suitable approximate solutions to these equations, especially the nonlinear class.

The traditional perturbation methods for solving FFDEs [13–16] have a significant disadvantage in that they are overly dependent on the presence of small parameters. This condition greatly affects perturbation methods' applications because most nonlinear equations do not even contain this small parameter. Moreover, determining small parameters is a complicated process and requires special techniques. Solving problems with approximate methods often helps to understand a physical problem better and may help to improve future procedures and designs used to solve these problems. The essential gain of an approximate method is the ability to solve difficult nonlinear problems without the need to compare them with the exact solution to determine the accuracy of the approximate solution. The approximate solution is acquired in the form of a series that converges quickly to the exact solution. A few approximate methods offer a simple way to ensure the solution.

Using similar methods to find solutions to these equations has its generous compensation, but not without obstacles. There should be more investigation of approximate methods for FFTBVPs that have yet to be applied.

The main focus of this work is to present a new formulation and analysis of the fuzzy fractional HAM (FF-HAM) from the crisp domain to the fuzzy environment to deal with linear and nonlinear FFTBVPs physical applications under the Caputo fractional sense. The HAM, like the previous methods that have been described, does not involve discretization of the variables and linearization; hence, is free from rounding off errors and does not require large computer memory or time. The method also provides the solution in a rapidly convergent series with elegantly computed components [17]. In his PhD thesis, Liao proposed the HAM, which is a powerful method for solving linear and nonlinear problems. Many researchers have recently used HAM to solve various linear and nonlinear problems in science and engineering. We refer the reader to Refs. [18–21]. An approximate method (of which HAM is an example) has an advantage over perturbation methods because it is not dependent on small or large parameters. Perturbation methods are based on the existence of small or large parameters, and they cannot be applied to all nonlinear equations. Again, according to Ref. [17], both perturbation and nonperturbative methods cannot provide a simple procedure to adjust or control the convergence region and rate of a given approximate series. One of the advantages of the HAM is that this method allows for fine-tuning of the convergence region and rate of convergence by enabling the convergence control parameter to vary. It is to be noted that proper choice of the initial guess, the auxiliary linear operator, and convergence control with the parameter will guarantee the convergence of the HAM solution series [20]. The HAM series solution will be convergent by considering two factors: the auxiliary linear operator and the initial guess.

The main properties of fuzzy sets, such as the fuzzy number and fuzzy extension principles, help us formulate our proposed method from a crisp environment to a fuzzy environment to find a reliable solution to FFDEs. Readers can look at the membership function [10], the-cut [22], fuzzy numbers [23], and the extension principle [24] to get different points of view on the fuzzy environment.

This paper aims to construct a new algorithm based on the HAM technique for solving fuzzy fractional boundary value problems and apply the algorithm to two physical models. Namely, the modeling of the motion of a rigid plate immersed in a Newtonian fluid and the distribution of the temperature in the lumped convection system in a layer comprised of materials with varying thermal conductivity. The contra-part of the fuzzy model for those problems is defined and solved via the new algorithm. The obtained solution is given in terms of a convergent series that contains a convergent control parameter which can be optimally chosen by minimizing the residual error , and this leads to an accurate solution to the problems.

The outline of this work is arranged as follows. In Section 2, we looked at several fundamental definitions and advanced ideas of the fractional calculus theory that will be useful in understanding the following parts of this research study. The fuzzy analysis and new formulation of FF-HAM for solving the purposed problem are discussed in Section 3, while the convergence of FF-HAM is illustrated analytically and summarized in the form of an algorithm in Section 4. Section 5 demonstrated and discussed the capabilities of the proposed FF-HAM in solving two application problems involving linear and nonlinear FFTBVPs. Finally, Section 6 concludes this study work.

2. Basic Concepts of Fuzzy Fractional Calculus

This section provides basic definitions of fractional calculus under the effect of uncertainty, which will help us deal with future procedures in this research paper.

Definition 1 (see [25]): For real number μ, and $x > 0$, the real function $y(x)$ is said to be in the space C_μ if $\exists p \in \mathbb{R}$ satisfies $y(x) = x^p y_1(x)$, where $y_1(x) \in C(0, \infty)$, whereas $y(x)$ is said to be in the space C_μ^m if $y^n \in C_\mu, m \in \mathbb{N}$, where $\mathbb{N}$ represents the set of natural numbers.

Definition 2 (see [25]): For any continuous fuzzy valued function $\widetilde{g}\in C^{\mathcal{F}}[a,b]\cap L^{\mathcal{F}}[a,b]$. The fuzzy fractional Riemann–Liouville integration of $\widetilde{g}(x)$ will be defined by

$$\mathcal{J}_0^{\rho}\widetilde{g}(x)=\frac{1}{\Gamma(\rho)}\int_0^x\widetilde{g}(y)(x-y)^{\rho-1}\mathrm{d}y,\quad \rho,x\in\mathbb{R},\ x>0. \tag{1}$$

$\forall\alpha\in[0,1]$, $\alpha-$ cuts for fuzzy valued function, and $\widetilde{g}$ can be represented by $\widetilde{g}(x;\alpha)=[g_l(x;\alpha),g_u(x;\alpha)]$, such that below are some of the fuzzy fractional Riemann–Liouville integration features:

(1) $\mathcal{J}_0^{0}\widetilde{g}(x;\alpha)=\widetilde{g}(x;\alpha)=[g_l(x;\alpha),g_u(x;\alpha)]$
(2) $\mathcal{J}_0^{\rho}x^s=\Gamma(s+1)/\Gamma(s+1+\rho)x^{s+\rho}$
(3) $\forall$ constant $r\in\mathbb{R}$, then $\mathcal{J}_0^{\rho}r=r/\Gamma(\rho+1)x^{\rho}$, $\beta>0$

Definition 3 (see [12, 26]): Let $\rho\in(1,2]$ and $\widetilde{g}\colon\ [a,b]\longrightarrow\widetilde{U}$ such that $\widetilde{g}$ and $\widetilde{g}'\in C^{\mathcal{F}}[0,b]\cap L^{\mathcal{F}}[0,b]$. Then we can define the fuzzy fractional derivative in the meaning of Caputo of the fuzzy function $\widetilde{g}$ at $x\in(a,b)$ as follows:

$$(D^{\rho}\widetilde{g})(x)=\frac{1}{\Gamma(2-\rho)}\int_0^x\frac{\widetilde{g}'(x)}{(y-x)^{\rho-1}}\mathrm{d}x,\quad x>0. \tag{2}$$

With the property [27], we get $\forall\ \rho>0$, then $D_0^{\rho}r=0$ for any constant $r\in\mathbb{R}$.

Here, $\Gamma(x)$ represents the Gamma function such that the Riemann–Liouville integral represents the left inverse operator of the Caputo fractional derivative [28].

3. Analysis of the FF-HAM for Second-Order FFTBVPs

According to the main structure of the HAM [28], we introduce a new approach based on HAM to solve second-order FFTBVPs. Consider the following inhomogeneous FFBVPs:

$$\begin{cases}\widetilde{y}^{(\rho)}(x)=\widetilde{g}(x,\widetilde{y}(x),\widetilde{y}\prime(x)),\widetilde{g}(x) & x\in[x_0,X],\\ \widetilde{y}(x_0)=\widetilde{a}_0,\ \widetilde{y}'(x_0)=\widetilde{a}_1,\\ \widetilde{y}(X)=\widetilde{b}_0,\ \widetilde{y}'(X)=\widetilde{b}_1,\\ \rho\in(1,2],\end{cases} \tag{3}$$

where $\widetilde{y}^{(\rho)}(x)$ is the fuzzy fractional derivative of order ρ, $\widetilde{y}(x)$ is the unknown fuzzy function, $\widetilde{a}_0,\widetilde{a}_1,\widetilde{b}_0,\widetilde{b}_1$ are the fuzzy numbers defined in Ref. [23], and $G(x)$ is the fuzzy inhomogeneous term. According to Ref. [10], we can construct the zeroth-order deformation equation of (3) as follows:

$$\begin{cases}(1-q)\underline{\mathcal{L}}_{\rho}\left[\left[\underline{y}(x;q)\right]_{\alpha}-\underline{y}_0(x;\alpha)\right]=q\,\underline{h}(\alpha)H(x)\left(\dfrac{\partial^{\rho}\left[\underline{y}(x;q)\right]_{\alpha}}{\partial x^{\rho}}-g_l([\widetilde{y}(x;q)]_{\alpha})-G(x;\alpha)\right),\\ \\ (1-q)\overline{\mathcal{L}}_{\rho}[[\overline{y}(x;q)]_{\alpha}-\overline{y}_0(x;\alpha)]=q\overline{h}(\alpha)H(x)\left(\dfrac{\partial^{\rho}\overline{y}[(x;q)]_{\alpha}}{\partial x^{\rho}}-g_u([\widetilde{y}(x;q)]_{\alpha})-G(x;\alpha)\right).\end{cases} \tag{4}$$

Here, $0\leq q\leq 1$ represents the embedding parameter, $\widetilde{h}(\alpha)=[\underline{h}(\alpha),\overline{h}(\alpha)]$ is a nonzero convergence control parameter, $H(x)$ is the auxiliary function, while the operators $\underline{\mathcal{L}}_{\rho}=\partial^{\rho}[\underline{y}(x;q)]_{\alpha}/\partial x^{\rho}$ and $\overline{\mathcal{L}}_{\rho}=\partial^{\rho}\overline{y}[(x;q)]_{\alpha}/\partial x^{\rho}$ are the auxiliary linear operators, and g_l,g_u are the lower and upper fuzzy functions, respectively. Now, for all α-level sets, we can define the initial approximation of the lower and upper bound $[\widetilde{y}_0(x)]_{\alpha}=[\underline{y}_0(x;\alpha),\overline{y}_0(x;\alpha)]$ by the rule of solution expression [29] as follows, from Equation (3), and the approximate solution $\widetilde{y}(x;\alpha)$ can be expressed for $k=0,1,2,\ldots$ by a set of base functions x^k, and then the approximate solution $\widetilde{y}(x;\alpha)$ can be expressed as $\widetilde{y}(x;\alpha)=\sum_{j=0}^{k}[\widetilde{d}^j]_{\alpha}x^j$, where $[\widetilde{d}^j]_{\alpha}$ are fuzzy coefficients to be determined. According to the rule of solution expression $\sum_{j=0}^{k}[\widetilde{d}^j]_{\alpha}x^j$, we have the following form of the fuzzy initial guess:

$$\begin{aligned}\underline{y}_0(x;\alpha)&=\underline{S}_1(\alpha)+\underline{S}_2(\alpha)x,\\ \overline{y}_0(x;\alpha)&=\overline{S}_1(\alpha)+\overline{S}_2(\alpha)x,\end{aligned} \tag{5}$$

where for all $\alpha\in[0,1]$,$\widetilde{S}_1(\alpha)$, and $\widetilde{S}_2(\alpha)$ are the constants that can be determined easily from the two-point boundary conditions in Equation (3). The two-point fuzzy boundary conditions of Equation (4) are

$$\begin{cases}[\widetilde{y}(x_0;q)]_{\alpha}=\widetilde{a}_0, & \dfrac{\partial}{\partial x}[\widetilde{y}(x_0;q)]_{\alpha}=\widetilde{a}_1,\\ \\ [\widetilde{y}(X;q)]_{\alpha}=\widetilde{b}_0, & \dfrac{\partial}{\partial x}[\widetilde{y}(X;q)]_{\alpha}=\widetilde{b}_1.\end{cases} \tag{6}$$

By setting $q=0$ and $q=1$, we have

$$\begin{aligned}&\begin{cases}\left[\underline{y}(x;0)\right]_{\alpha}=\underline{y}(x_0;\alpha),\\ [\overline{y}(x;0)]_{\alpha}=\overline{y}(x_0;\alpha),\end{cases}\\ &\begin{cases}\left[\underline{y}(x;1)\right]_{\alpha}=\underline{Y}(x;\alpha),\\ [\overline{y}(x;1)]_{\alpha}=\overline{Y}(x;\alpha).\end{cases}\end{aligned} \tag{7}$$

At a time when the embedding parameter changes from zero to one, the fuzzy solution $[\widetilde{y}(x;q)]_{\alpha}$ deforms from the initial approximation $[\widetilde{y}(x;0)]_{\alpha}$ to the exact solution

$\widetilde{Y}(x;\alpha)$. Now by expanding the approximate solution $[\widetilde{y}(x;q)]_\alpha$ as a Taylor series with respect to q, $\forall\alpha \in [0,1]$, we have

$$\left\{ \left[\underline{y}(x;q)\right]_\alpha = \underline{y}_0(x;\alpha) + \sum_{j=1}^{\infty} \underline{y}_j(x;\alpha)q^j, \ [\overline{y}(x;q)]_\alpha = \overline{y}_0(x;\alpha) + \sum_{j=1}^{\infty} \overline{y}_j(x;\alpha)q^j, \right. \tag{8}$$

where

$$\begin{cases} \underline{y}_j(x;\alpha) = \dfrac{1}{j!}\dfrac{\partial^j\left[\underline{y}(x;q)\right]_\alpha}{\partial q^j}\Big|_{q=0}, \\ \overline{y}_j(x;\alpha) = \dfrac{1}{j!}\dfrac{\partial^j[\overline{y}(x;q)]_\alpha}{\partial q^j}\Big|_{q=0}. \end{cases} \tag{9}$$

If the auxiliary linear operator $\widetilde{\mathscr{L}}_\rho$, the initial guess $\widetilde{y}_0(x;\alpha)$ and the convergence control parameter $\widetilde{h}(\alpha)$ are properly chosen, and it fixed the auxiliary function $H(x) = 1$, the FF-HAM series solution will converge to the exact solution at $q = 1$ such that

$$\left\{ \underline{Y}(x;\alpha) = \underline{y}_0(x;\alpha) + \sum_{j=1}^{\infty} \underline{y}_j(x;\alpha), \overline{Y}(x;\alpha) = \overline{y}_0(x;\alpha) + \sum_{j=1}^{\infty} \overline{y}_j(x;\alpha). \right. \tag{10}$$

In most cases, it is impossible to find the analytical solution with the FF-HAM as an infinite series, especially for nonlinear FFBVPs, and this brings us to defining the vectors

$$\left\{ \overrightarrow{\underline{y}}_j(x;\alpha) = \left\{\underline{y}_0(x;\alpha), \underline{y}_1(x;\alpha), \ldots, \underline{y}_k(x;\alpha)\right\}, \overrightarrow{\overline{y}}_j(x;\alpha) = \left\{\overline{y}_0(x;\alpha), \overline{y}_1(x;\alpha), \ldots, \overline{y}_k(x;\alpha)\right\}. \right. \tag{11}$$

Now by differentiating the zeroth-order deformation equation k times with respect to the embedding parameter q is followed by setting $q = 0$, after that dividing them by $k!$ to extract the k^{th} order deformation equation is as follows:

$$\begin{cases} \dfrac{\partial^\rho}{\partial x^\rho}\left[\underline{y}_k(x;\alpha) - \psi_k \underline{y}_{k-1}(x;\alpha)\right] = \underline{h}(\alpha)\mathscr{R}_k\left(\overrightarrow{\underline{y}}_{k-1}(x;\alpha)\right), \\ \dfrac{\partial^\rho}{\partial x^\rho}\left[\overline{y}_k(x;\alpha) - \psi_k \overline{y}_{k-1}(x;\alpha)\right] = \overline{h}(\alpha)\mathscr{R}_k\left(\overrightarrow{\overline{y}}_{k-1}(x;\alpha)\right), \end{cases} \tag{12}$$

where

$$\begin{cases} \mathscr{R}_k\left(\overrightarrow{\underline{y}}_{k-1}(x;\alpha)\right) = \dfrac{1}{(k-1)!}\dfrac{\partial^{k-1}\left(\left(\partial^\rho\left[\underline{y}(x;q)\right]_\alpha/\partial x^\rho\right) - g_l\left([\widetilde{y}(x;q)]_\alpha\right) - \overrightarrow{\underline{y}}_{k-1}(x;\alpha)\right)}{\partial q^{k-1}}\Big|_{q=0}, \\ \mathscr{R}_k\left(\overrightarrow{\overline{y}}_{k-1}(x;\alpha)\right) = \dfrac{1}{(k-1)!}\dfrac{\partial^{k-1}\left(\left(\partial^\rho\overline{y}[(x;q)]_\alpha/\partial x^\rho\right) - g_u\left([\widetilde{y}(x;q)]_\alpha\right) - \overrightarrow{\overline{y}}_{k-1}(x;\alpha)\right)}{\partial q^{k-1}}\Big|_{q=0}. \end{cases} \tag{13}$$

The solution of the k^{th} order deformation for $k \geq 1$ is

$$\begin{cases} \underline{y}_k(x;\alpha) = \underline{y}_k(x_0;\alpha) + \underline{y}_k'(x_0;\alpha)x \\ +\psi_k\left(\underline{y}_{k-1}(x;\alpha) - \underline{y}_{k-1}(x_0;\alpha) - \underline{y}_{k-1}'(x_0;\alpha)x\right) + \underline{h}(\alpha)\underline{\mathcal{J}}^{(\rho)}\mathcal{R}_k\left(\underline{\vec{y}}_{k-1}(x;\alpha)\right), \\ \overline{y}_k(x;\alpha) = \overline{y}_k(x_0;\alpha) + \overline{y}_k'(x_0;\alpha)x \\ +\psi_k\left(\overline{y}_{k-1}(x;\alpha) - \overline{y}_{k-1}(x_0;\alpha) - \overline{y}_{k-1}'(x_0;\alpha)x\right) + \overline{h}(\alpha)\overline{\mathcal{J}}^{(\rho)}\mathcal{R}_k\left(\overline{\vec{y}}_{k-1}(x;\alpha)\right). \end{cases} \tag{14}$$

$\psi_k = \begin{cases} 0, & k \leq 1, \\ 1, & k > 1. \end{cases}$ and $\tilde{\mathcal{J}}^{\rho} = [\underline{\mathcal{J}}^{\rho}, \overline{\mathcal{J}}^{\rho}] = \tilde{\mathcal{L}}_{\rho}^{-1}$ are the fuzzy Riemann–Liouville integrals of order $\rho \in (1, 2]$.

Finally, the k^{th}-order of the series solution becomes

$$\tilde{Y}_k = \left\{ \underline{Y}(x;\alpha) = \underline{y}_0(x;\alpha) + \sum_{j=1}^{k} \underline{y}_j(x;\alpha), \overline{Y}(x;\alpha) = \overline{y}_0(x;\alpha) + \sum_{j=1}^{k} \overline{y}_j(x;\alpha). \right. \tag{15}$$

4. Convergence Analysis Algorithm of the FF-HAM

In this section, we will present the convergence dynamic of FF-HAM based on the residual of Equation (3) to figure out the best optimal convergence control parameter $\tilde{h}$ to find a reliable approximate solution via the FF-HAM.

The perfect selection of the convergence control parameter $\tilde{h}$ would ensure the convergence of the FF-HAM series solution. Following the HAM that was introduced in Ref. [28]and the series approximate solution of order k in Equation (6), we can conclude that the main feature of HAM lies in control, and modify the convergence of series solution in view of existing the convergence control parameter $\tilde{h}$ [30] based on the minimum residual of Equation (3). Here, the optimal convergence control parameter $\tilde{h}$ can be determined based on the residual formula of Equation (3) as follows:

$$\begin{cases} \underline{\mathrm{ER}}(x;\alpha;\underline{h}) = \underline{y}^{(\rho)}(x;\alpha;\underline{h}) - g_l(x, \tilde{y}(x;\alpha;\tilde{h})) - \underline{G}(x;\alpha), \\ \overline{\mathrm{ER}}(x;\alpha;\overline{h}) = \overline{y}^{(\rho)}(x;\alpha;\overline{h}) - g_u(x, \tilde{y}(x;\alpha;\tilde{h})) - \overline{G}(x;\alpha). \end{cases} \tag{16}$$

Now, $\forall \alpha \in [0, 1]$, then we will check the corresponding squared residual error, followed by integrating the residual over the given interval $x \in [x_0, X]$, then we obtain the form as follows:

$$\begin{cases} \underline{\mathrm{SER}}(x;\alpha;\underline{h}) = \int_{x_0}^{X} [\underline{\mathrm{ER}}(x;\alpha;\underline{h})]^2 \mathrm{d}x, \\ \overline{\mathrm{SER}}(x;\alpha;\overline{h}) = \int_{x_0}^{X} [\overline{\mathrm{ER}}(x;\alpha;\overline{h})]^2 \mathrm{d}x. \end{cases} \tag{17}$$

By setting the values of fractional order $1 < \rho \leq 2$, then the following partial derivatives with respect to $\tilde{h}(\alpha)$ can be obtained for all $\alpha \in [0, 1]$ as

$$\frac{\partial \widetilde{\mathrm{SER}}(x;\alpha;\tilde{h}(\alpha))}{\partial \tilde{h}(\alpha)} = 0 \longrightarrow \begin{cases} \dfrac{\partial \underline{\mathrm{SER}}(x;\alpha;\underline{h}(\alpha))}{\partial \underline{h}(\alpha)} = 0, \\ \dfrac{\partial \overline{\mathrm{SER}}(x;\alpha;\overline{h}(\alpha))}{\partial \overline{h}(\alpha)} = 0. \end{cases} \tag{18}$$

The main feature of the FF-HAM approach lies in identifying the valid region of $\tilde{h}$ which makes $\widetilde{\mathrm{SER}}(x;\tilde{h};\alpha)$ trending towards zero in conjunction with the increasing FF-HAM series order in a way identifying the optimum value of $\tilde{h}(\alpha)$ which is linked with the minimum value of the residual of Equation (3), where in our proposed FF-HAM, we will obtain the optimum value of $\tilde{h}(\alpha)$ by setting $\widetilde{\mathrm{SER}}(x;\alpha;\tilde{h}) = 0$ via the NSolve Mathematica 12 package. Finally, $\forall \alpha \in [0, 1]$, then we will estimate the best value of $\tilde{h}(\alpha)$ for the convergence of the approximate FF-HAM series solution $\tilde{y}(x;\alpha;\tilde{h})$. We are seeking for region S of the optimum values of $\tilde{h}(\alpha)$ i.e., $(\tilde{h}(\alpha) \in S)$, where this region almost matched the parallel line segment to the x-axis. In our proposed approach for linear and nonlinear FFTBVP of the second order, we have to plot $\tilde{h}$-curve $\forall \alpha \in [0, 1]$ stages and select the $\alpha-$ level set that provides us the convergence series solution for all level sets, say we fix $\alpha = \alpha_0$. After that, we can plot $\tilde{y}^{(\rho)}(x;\alpha_0;\tilde{h})$ for different order $\rho \in (1, 2]$ for the lower and the upper bound of the approximate solution $\tilde{y}(x;\alpha;\tilde{h})$ of Equation (3) and apply this optimum value $\tilde{h}(\alpha_0)$ for each level set approximate solutions. Finally, the steps in the FF-HAM algorithm for finding an approximate solution to Equation (3) are described as follows:

Step 1: Set fractional order $\rho \in (1, 2]$

Step 2: Set the fuzzy initial approximation $\tilde{y}_0(x;\alpha)$

Step 3: Set the value of the fuzzy inhomogeneous term $\tilde{G}(x;\alpha)$

Step 4: Set the number of terms, such that $j = 1, 2, 3, \ldots, k$

Step 5: Set $j = j + 1$, and for $j = 1$ to $j \le k$, evaluate

$$\tilde{y}_j(x;\alpha) = \underline{y}_j(x_0;\alpha) + \underline{y}_j'(x_0;\alpha)x + \psi_j\left(\tilde{y}_{j-1}(x;\alpha) - \underline{y}_{j-1}(x_0;\alpha) - \underline{y}_{j-1}'(x_0;\alpha)x\right) + \tilde{h}(\alpha)\left(\tilde{y}_{j-1}(x) - \tilde{\mathcal{J}}^{\rho}\tilde{g}(x,\tilde{y}(x),\tilde{y}\prime(x)) - \tilde{\mathcal{J}}^{\rho}\tilde{G}(x)\right). \quad (19)$$

Step 6: Compute the fuzzy series of order K: $\tilde{y}(x;\alpha;\tilde{h}) = \sum_{j=0}^{K}\tilde{y}_j(x;\alpha;\tilde{h})$

Step 7: Plot $\tilde{h}(\alpha_0)$– curve over the interval $\tilde{h}(\alpha_0) \in [-2,1]$

Step 8: Set the residual of the given FFBVP (Equation (3)) as shown in Equation (16) followed by using Equations (17) and (18) in order to determine the valid region of the optimal convergence control parameter in the valid region showed in the previous step, followed by detecting the best optimal convergence control parameter $\tilde{h}_{\text{opt}}(\alpha_0)$

Step 9: Utilize the best optimal value of the convergence control parameter $\tilde{h}_{\text{opt}}(\alpha_0)$ in the approximate series in Step 5 for lower and upper bound $\forall\alpha \in [0,1]$

5. Applications and Results

Using the method, we suggested in Sections 3 and 4, we look at how well Equation (3) approximate solutions are implemented and checked. We use the following linear and nonlinear FFBVPs physical problems to do this.

Problem 1. Bagley–Torvik equation

Consider the fuzzy fractional Bagley–Torvik equation [9]:

$$D^{(1.5)}\tilde{y}(x) + \tilde{y}(x) = \tilde{F}(x;\alpha), \quad x \in [0,1]. \quad (20)$$

Such that

$$\tilde{F}(x;\alpha) = \left(\underline{F}(x;\alpha), \overline{F}(x;\alpha)\right) = \left(\alpha\left(x^2 - x\right) + 4\alpha\frac{\sqrt{x}}{\sqrt{\pi}}, (2-\alpha)\left(x^2 - x\right) + 4(2-\alpha)\frac{\sqrt{x}}{\sqrt{\pi}}\right). \quad (21)$$

That is subject to the following fuzzy boundary condition:

$$\begin{cases} \underline{y}(0;\alpha) = \underline{y}(1;\alpha) = (\alpha - 1), \\ \overline{y}(0;\alpha) = \overline{y}(1;\alpha) = (1-\alpha). \end{cases} \quad (22)$$

This equation arises in the modelling of the motion of a rigid plate immersed in a Newtonian fluid. The motion of a rigid plate of mass m and area A connected by a mass less spring of stiffness k is immersed in a Newtonian fluid, such that Figure 1 illustrates the dynamics of Bagley–Torvik equation.

With the following fuzzy exact solution [9], we get

$$\begin{cases} \underline{Y}(x;\alpha) = \alpha\left(x^2 - x\right), \\ \overline{Y}(x;\alpha) = (2-\alpha)\left(x^2 - x\right). \end{cases} \quad (23)$$

According to the FF-HAM analysis section, we construct the k^{th}-order deformation equations for $k \ge 1$ of Equation (20) as follows:

$$\begin{cases} \underline{y}_k(x;\alpha) = (1-\alpha) \\ +\psi_k\left(\underline{y}_{k-1}(x;\alpha) - (1-\alpha)\right) + \underline{h}(\alpha)\underline{\mathcal{J}}^{(\rho)}\mathcal{R}_k\left(\underline{\vec{y}}_{k-1}(x;\alpha)\right), \\ \overline{y}_k(x;\alpha) = (\alpha - 1) \\ +\psi_k\left(\overline{y}_{k-1}(x;\alpha) - (\alpha-1)\right) + \overline{h}(\alpha)\overline{\mathcal{J}}^{(\rho)}\mathcal{R}_k\left(\overline{\vec{y}}_{k-1}(x;\alpha)\right). \end{cases} \quad (24)$$

Then $\underline{y}_k(0;\alpha) = 0, \overline{y}_k(0;\alpha) = 0$ and $\underline{y}_k(1;\alpha) = 0, \overline{y}_k(1;\alpha) = 0$ such that

$$\psi_k = \begin{cases} 0, & k \le 1, \\ 1, & k > 1, \end{cases}$$
$$\cdot \begin{cases} \mathcal{R}_k\left(\underline{\vec{y}}_{k-1}(x;\alpha)\right) = \underline{y}_{k-1}^{(1.5)}(x;\alpha) + \underline{y}_{k-1}(x;\alpha) - (1-\psi_k)\underline{F}(x;\alpha), \\ \mathcal{R}_k\left(\overline{\vec{y}}_{k-1}(x;\alpha)\right) = \overline{y}_{k-1}^{(1.5)}(x;\alpha) + \overline{y}_{k-1}(x;\alpha) - (1-\psi_k)\overline{F}(x;\alpha), \end{cases} \quad (25)$$

where $D^{(1.5)}y = y^{(1.5)}$. Then we can choose the initial guess as

$$\tilde{y}_0(x;\alpha) = [1-\alpha, \alpha - 1]. \quad (26)$$

Expanding Equation (25) we get those as follows:

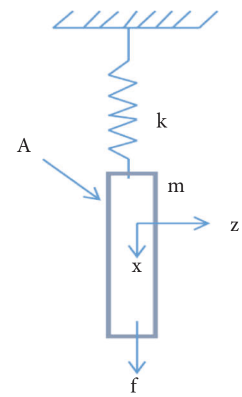

Figure 1: Rigid plate of mass m immersed into a Newtonian fluid.

For $k = 1$, we have

$$\begin{cases} \underline{y}_1(x;\alpha) = (1-\alpha) + \underline{h}(\alpha)\underline{\mathcal{J}}^{(1.5)}\left(\underline{y}_0^{(1.5)}(x;\alpha) + \underline{y}_0(x;\alpha) - \underline{F}(x;\alpha)\right), \\ \overline{y}_1(x;\alpha) = (\alpha-1) + \overline{h}(\alpha)\overline{\mathcal{J}}^{(1.5)}\left(\overline{y}_0^{(1.5)}(x;\alpha) + \overline{y}_0(x;\alpha) - \overline{F}(x;\alpha)\right). \end{cases} \quad (27)$$

For $k = 2$, we have

$$\begin{cases} \underline{y}_2(x;\alpha) = (1-\alpha) + \left(\underline{y}_1(x;\alpha) - (1-\alpha)\right) + \underline{h}(\alpha)\underline{\mathcal{J}}^{(1.5)}\left(\underline{y}_1^{(1.5)}(x;\alpha) + \underline{y}_1(x;\alpha)\right), \\ \overline{y}_2(x;\alpha) = (\alpha-1) + (\overline{y}_1(x;\alpha) - (\alpha-1)) + \overline{h}(\alpha)\overline{\mathcal{J}}^{(1.5)}\left(\overline{y}_1^{(1.5)}(x;\alpha) + \overline{y}_1(x;\alpha)\right). \end{cases} \quad (28)$$

For $k = 3$, we have

$$\begin{cases} \underline{y}_3(x;\alpha) = (1-\alpha) + \left(\underline{y}_2(x;\alpha) - (1-\alpha)\right) + \underline{h}(\alpha)\underline{\mathcal{J}}^{(1.5)}\left(\underline{y}_2^{(1.5)}(x;\alpha) + \underline{y}_2(x;\alpha)\right), \\ \overline{y}_3(x;\alpha) = (\alpha-1) + (\overline{y}_2(x;\alpha) - (\alpha-1)) + \overline{h}(\alpha)\overline{\mathcal{J}}^{(1.5)}\left(\overline{y}_2^{(1.5)}(x;\alpha) + \overline{y}_2(x;\alpha)\right). \end{cases} \quad (29)$$

Then for general k, we have

$$\begin{cases} \underline{y}_k(x;\alpha) = (1-\alpha) + \left(\underline{y}_{k-1}(x;\alpha) - (1-\alpha)\right) + \underline{h}(\alpha)\underline{\mathcal{J}}^{(1.5)}\left(\underline{y}_{k-1}^{(1.5)}(x;\alpha) + \underline{y}_{k-1}(x;\alpha)\right), \\ \overline{y}_k(x;\alpha) = (\alpha-1) + (\overline{y}_{k-1}(x;\alpha) - (\alpha-1)) + \overline{h}(\alpha)\overline{\mathcal{J}}^{(1.5)}\left(\overline{y}_{k-1}^{(1.5)}(x;\alpha) + \overline{y}_{k-1}(x;\alpha)\right). \end{cases} \quad (30)$$

The third-order FF-HAM approximate series solution uses the Mathematica 12 package to find the solutions for the lower and for the upper bounds, and we obtain the following form:

$$\left\{ \underline{y}(x;\alpha;\underline{h}) = \underline{y}_0(x;\alpha) + \sum_{j=1}^{3}\underline{y}_j(x;\alpha;\underline{h}), \overline{y}(x;\alpha;\overline{h}) = \overline{y}_0(x;\alpha) + \sum_{j=1}^{3}\overline{y}_j(x;\alpha;\overline{h}). \right. \quad (31)$$

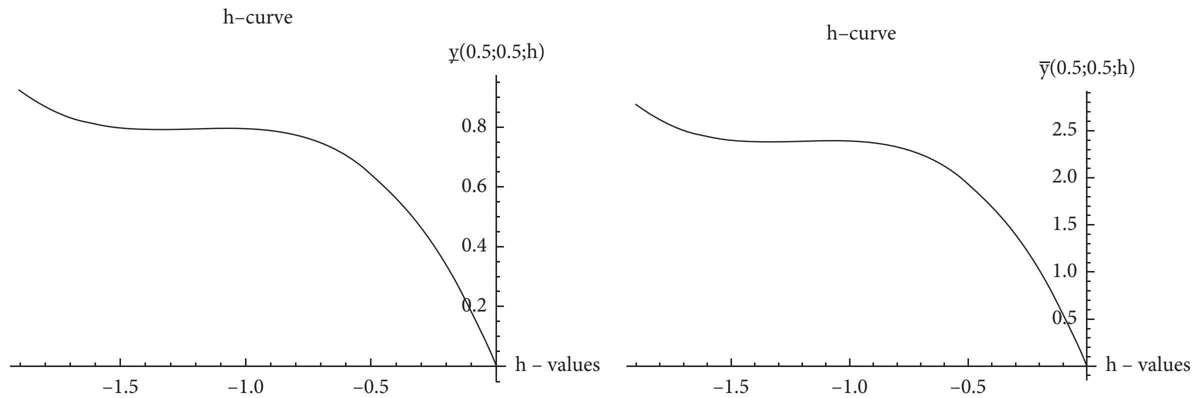

Figure 2: The $\tilde{h}$-curve of Equation (20) for the third-order FF-HAM approximate solution when $H(x) = 1$.

We can show the accuracy of FF-HAM for solving Equation (20) by taking the residual error as mentioned in Equation (16) such that

$$\begin{cases} \underline{\mathrm{ER}}\,(x;\alpha;\underline{h}) = \left(\underline{y}^{(1.5)}(x;\alpha) + \underline{y}(x;\alpha) - \underline{F}(x;\alpha)\right), \\ \overline{\mathrm{ER}}(x;\alpha;\overline{h}) = \left(\overline{y}^{(1.5)}(x;\alpha) + \overline{y}(x;\alpha) - \overline{F}(x;\alpha)\right). \end{cases} \quad (32)$$

As we mentioned in Section 3, this series depends upon x, α and the convergent control parameter $\tilde{h}$. According to Section 2, the convergent control parameter $\tilde{h}$ can be employed to adjust the convergence region of the FF-HAM, then we use the properties of FF-HAM convergence to find the best value of $\tilde{h}$. Toward this end, for fixed value of $0 \le \alpha \le 1$, say $\alpha = 0.5$, we plotted the $\tilde{h}$ -curve of the lower bound and upper bound via the third-order FF-HAM for Equation (20), as summarized in Figure 2.

According to the above curves in Figure 2, it is easy to discover the valid region of $\tilde{h}(0.5)$ which corresponds to the line segment nearly parallel to the horizontal axis such that the FF-HAM series solution is convergent when $-1.5 \le \tilde{h} \le -0.8$, and the best value of h can be obtained by minimizing the square residual error $\widetilde{\mathrm{SER}}(x;0.5;\tilde{h}) = [\underline{\mathrm{SER}}\,(x;0.5;\underline{h}), \overline{\mathrm{SER}}(x;0.5;\overline{h})]$ (we solve $\partial\widetilde{\mathrm{SER}}(x;0.5;\tilde{h}(0.5))/\partial\tilde{h}(0.5) = 0$), which yields $\tilde{h} = -1.0488155053478476$. Therefore, we have tabulated the residual errors $[\underline{\mathrm{ER}}]_\alpha$ and $[\mathrm{ER}]_\alpha$ of the approximate solutions $\underline{y}(0.5;\tilde{h};0.5)$ and $\overline{y}(0.5;\tilde{h};0.5)$ obtained by using the third-order FF-HAM in Table 1.

Table 1 illustrates the lower and upper solutions of Equation (20) using the third-order FF-HAM based on the best optimal convergence control parameter $\tilde{h} = -1.0488155053478476$. We can also summarize the solutions as overall $x \in [0, 0.5]$ and $\alpha \in [0, 1]$ corresponding with the best optimal convergence control value of $\tilde{h}$ for Equation (20), as shown in Figure 2.

For studying the behavior of FF-HAM for solving second-order FFTBVPs, we shall proceed to solve Equation (20) via the FF-HAM at the same given $x \in [0, 0.5]$ and $\rho = 1.5$ of order five instead of order three to analyze the convergency dynamic of FF-HAM for different terms of the series approximate solution. Beginning with identifying the valid region of the convergence control parameters of the fifth-order FF-HAM is summarized in Figure 3.

Table 1: The accuracy of lower and upper solutions of Equation (20) via the third-order FF-HAM when $\rho = 1.5$ at $x = 0.5$ for $\alpha \in [0, 1]$.

α	$[\underline{\mathbf{ER}}]_\alpha, \tilde{\mathbf{h}}$	$[\overline{\mathbf{ER}}]_\alpha, \tilde{\mathbf{h}}$	$[\underline{\mathbf{y}}]_\alpha, \tilde{\mathbf{h}}$	$[\overline{\mathbf{y}}]_\alpha, \tilde{\mathbf{h}}$
0	2.02950×10^{-4}	0	−0.50005	0
0.2	1.82655×10^{-4}	2.02950×10^{-5}	−0.45004	−0.05000
0.4	1.62360×10^{-4}	4.05901×10^{-5}	−0.40004	−0.10001
0.6	1.42065×10^{-4}	6.08852×10^{-5}	−0.35003	−0.15001
0.8	1.21770×10^{-4}	8.11802×10^{-5}	−0.30003	−0.20002
1	1.01475×10^{-4}	1.01475×10^{-4}	−0.25002	−0.25002

From Figure 3, it is easy to conclude that the valid region of the convergence control parameters that corresponds to the line segment nearly parallel to the horizontal axis has changed to $-1.5 \le \tilde{h} \le -0.5$ after changing the order of the FF-HAM, and then the best value of the convergent control parameter is $\tilde{h} = -1.0549896423027272$. In the next table, we have tabulated the residual errors $[\underline{\mathrm{ER}}]_\alpha$ and $[\overline{\mathrm{ER}}]_\alpha$ of the approximate solutions $\underline{y}(0.5;\tilde{h};\alpha)$ and $\overline{y}(0.5;\tilde{h};\alpha)$ obtained by using the fifth-order FF-HAM.

We can also summarize the solutions via the fifth-order FF-HAM overall $x \in [0, 0.5]$ and $\alpha \in [0, 1]$ corresponding with the best optimal convergence control values $\tilde{h}$ of Equation (20) in the following three-dimensional Figure 4.

In Tables 1 and 2, Figures 4 and 5 illustrate that the third and fifth-order FF-HAM satisfies the triangular solution of the fuzzy differential equations [23] for Equation (20). On the other hand, we can conclude that the solution accuracy of Equation (20) via the FF-HAM will approach the exact solutions whenever the order of FF-HAM series increases. One can explore Figures 6 and Figure 7 that illustrate the accuracy of fifth-order FF-HAM compared with the fifth-order Matern method (M6) [9] for solving Equation (20), where $\forall x \in [0, 1]$ for $\alpha = 0.5$ which is based on the absolute error of Equation (20) as follows:

$$\begin{cases} \underline{\mathrm{ERR}}\,(x;\alpha;\underline{h}) = \left|\underline{y}(x;\alpha;\underline{h}) - \underline{Y}(x)\right|, \\ \overline{\mathrm{ERR}}(x;\alpha;\overline{h}) = |\overline{y}(x;\alpha;\overline{h}) - \overline{Y}(x)|. \end{cases} \quad (33)$$

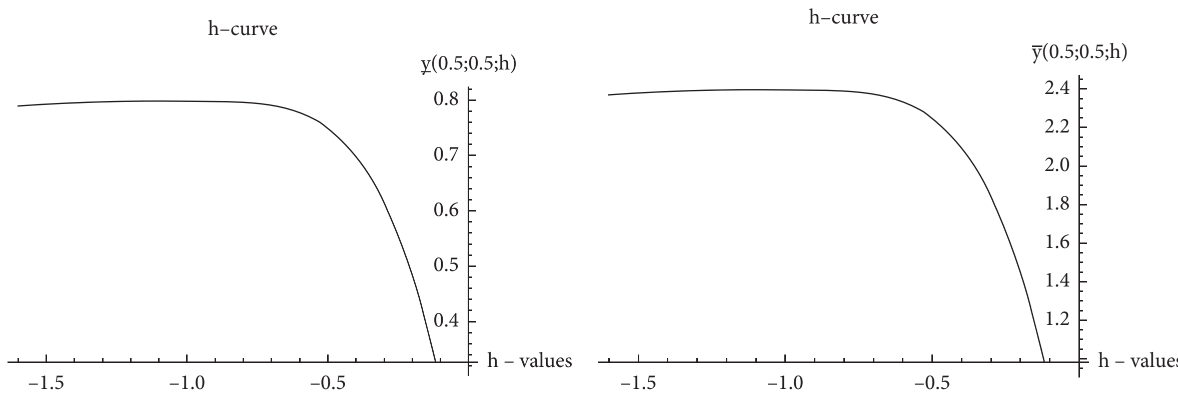

Figure 3: The $\tilde{h}$-curve of Equation (20) for the fifth-order FF-HAM approximate solution when $H(t) = 1$.

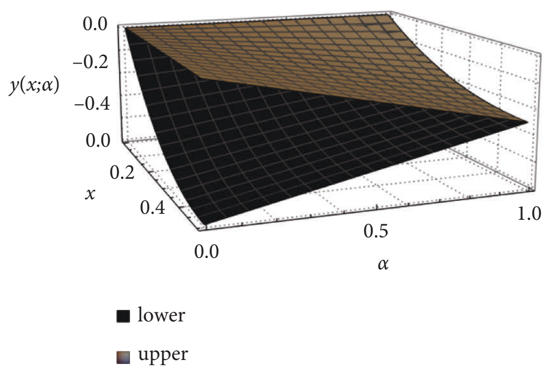

Figure 4: Three-dimensional fifth-order FF-HAM corresponding to the best optimal convergence control parameter $\tilde{h}(0.5)$ for all $x \in [0, 0.5]$ at $\rho = 1.5$ and for all $\alpha \in [0, 1]$.

We can conclude from Figures 6 and 7 that the accuracy of the approximate solution solved by the fifth-order FF-HAM series gives a better approximate compared with the Matern method (M6) [9] for all $x \in [0, 1]$.

Problem 2. Nonlinear Fractional Temperature Distribution Equation [31].

Consider the following mathematical model of order $\rho \in (1, 2]$ [31], which explains the distribution of the temperature in the lumped convection system in a layer comprised of materials with varying thermal conductivity as

$$D^{(\rho)} y(x) - \eta (y(x))^4 = 0, \quad x \in [0, 1]. \tag{34}$$

Subject to the following boundary conditions as

$$y'(0) = 0, \quad y(1) = 1, \tag{35}$$

where x is the time-independent variable, and $y(x)$ is the dimensionless temperature.

The fuzzy version of Equation (34) will be

Table 2: The accuracy of the lower and upper solution of Equation (20) via the fifth-order FF-HAM when $\rho = 1.5$ at $x = 0.5$ for $\alpha \in [0, 1]$.

α	$[\underline{\mathbf{ER}}]_\alpha, \tilde{\mathbf{h}}$	$[\overline{\mathbf{ER}}]_\alpha, \tilde{\mathbf{h}}$	$[\underline{\mathbf{y}}]_\alpha, \tilde{\mathbf{h}}$	$[\overline{\mathbf{y}}]_\alpha, \tilde{\mathbf{h}}$
0	4.20230×10^{-7}	0	−0.49999	0
0.2	3.78206×10^{-7}	4.20229×10^{-8}	−0.44999	−0.04999
0.4	3.36183×10^{-7}	8.40458×10^{-8}	−0.39999	−0.09999
0.6	2.94160×10^{-7}	1.26069×10^{-7}	−0.34999	−0.14999
0.8	2.52138×10^{-7}	1.68092×10^{-7}	−0.29999	−0.19999
1	2.10115×10^{-7}	2.10115×10^{-7}	−0.24999	−0.24999

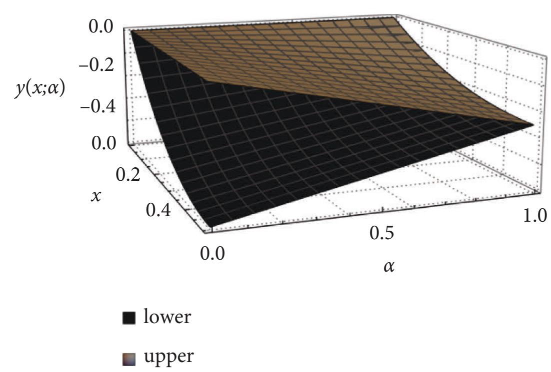

Figure 5: Three-dimensional third-order FF-HAM corresponding to the best optimal convergence control parameter $\tilde{h}(0.5)$ for all $x \in [0, 0.5]$ at $\rho = 1.5$ and for all $\alpha \in [0, 1]$.

$$\begin{cases} D^{(\rho)} \tilde{y}(x;\alpha) - \eta (y(x;\alpha))^4 = 0, \\ x \in [0, 1], \\ y'(0;\alpha) = (0.1\alpha - 0.1), \\ \underline{yy}(1;\alpha) = (0.1\alpha + 0.9), \\ \overline{y}'(0;\alpha) = (0.1 - 0.1\alpha), \\ \overline{y}(1;\alpha) = (1.1 - 0.1\alpha). \end{cases} \tag{36}$$

According to Section 3, we construct the zeroth order and k^{th}-order deformation equations for $k \geq 1$ of Equation (36) as follows:

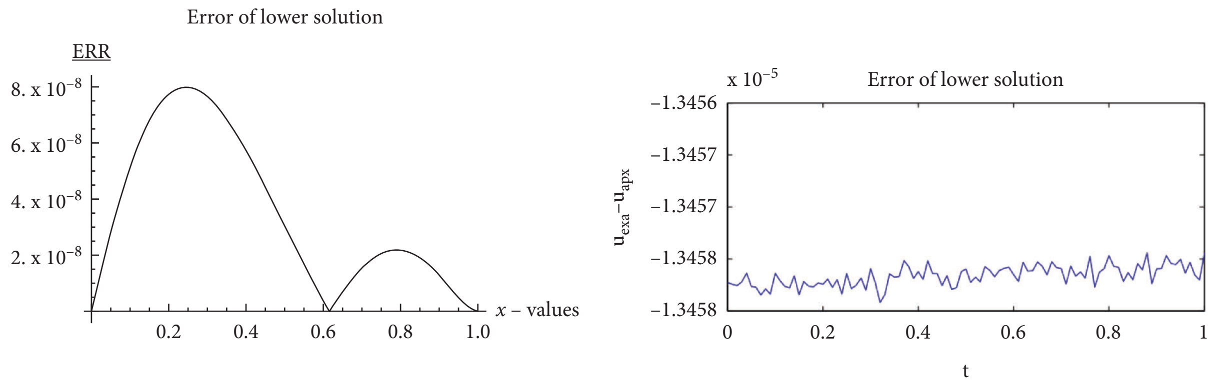

Figure 6: Lower bound accuracy of Equation (20) via the fifth-order FF-HAM and fifth-order M6 for $\alpha = 0.5$ and $x \in [0, 1]$.

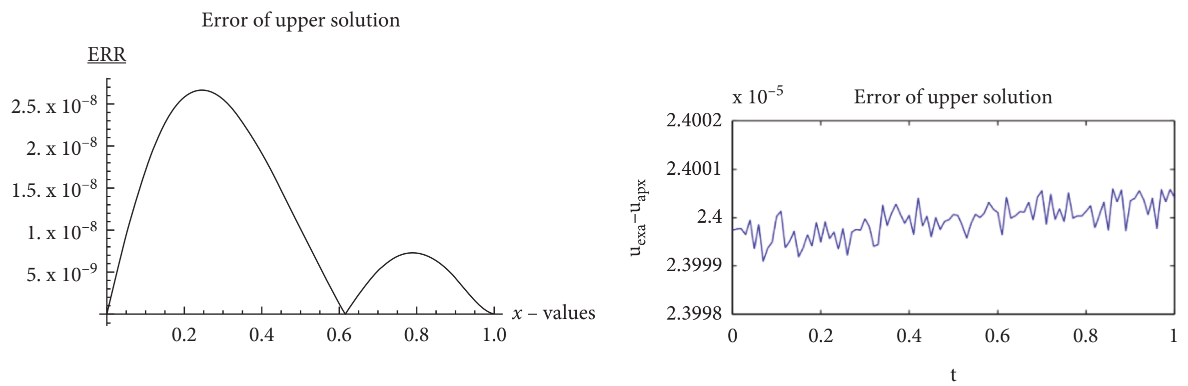

Figure 7: Upper bound accuracy of Equation (20) via the fifth-order FF-HAM and fifth-order M6 for $\alpha = 0.5$ and $x \in [0, 1]$.

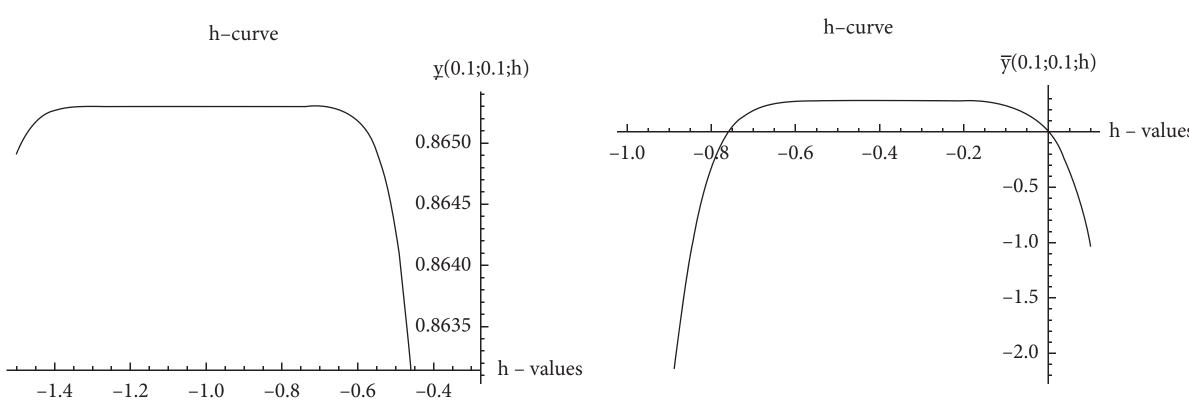

Figure 8: The $\tilde{h}$-curve of Equation (36) for the tenth-order FF-HAM approximate solution when $H(x) = 1$.

$$\begin{cases} \tilde{y}_k(x;\alpha) = [1-(0.1-0.1\alpha)x, 1+(0.1-0.1\alpha)x] \\ +\psi_k\left(\tilde{y}_{k-1}(x;\alpha) - [1-(0.1-0.1\alpha)x, 1+(0.1-0.1\alpha)x]\right) \\ +\tilde{h}(\alpha)\,\tilde{\mathcal{J}}^{(\beta_1)}\mathcal{R}_k\left(\overrightarrow{\tilde{y}_{k-1}}(x;\alpha)\right), \\ \underline{y}'(0;\alpha) = (0.1\alpha - 0.1), \underline{y}(1;\alpha) = (0.1\alpha + 0.9), \\ \overline{y}'(0;\alpha) = (0.1 - 0.1\alpha), \overline{y}(1;\alpha) = (1.1 - 0.1\alpha). \end{cases} \tag{37}$$

Such that

$$\psi_k = \begin{cases} 0, & k \le 1, \\ 1, & k > 1. \end{cases} \tag{38}$$

We noted that the nonlinear term of the form $y^4(x;\alpha)$ can be expanded by the Taylor series about the embedding parameter q as

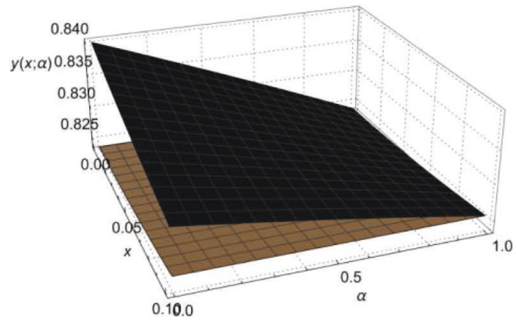

Figure 9: Three-dimensional third-order FF-HAM corresponding to the optimal convergence control parameter $\tilde{h}$ for all $x \in [0, 0.1]$ at $\rho = 1.9$, for $\eta = 0.6$, and for all $\alpha \in [0, 1]$.

$$y^4(x;\alpha;q) = \left(\sum_{k=0}^{\infty} y_k q^k\right)^4 = \sum_{k=0}^{\infty}\left(\sum_{i=0}^{k} y_{k-i}\sum_{j=0}^{i} y_{i-j}\sum_{s=0}^{j} y_s y_{j-s}\right)q^k. \tag{39}$$

Table 3: The accuracy of the lower and upper solution of Equation (36) via the tenth-order FF-HAM when $\rho = 1.9$ at $x = 0.1$ for $\alpha \in [0, 1]$.

α	$[\underline{\mathbf{ER}}]_\alpha, \tilde{\mathbf{h}}$	$[\overline{\mathbf{ER}}]_\alpha, \tilde{\mathbf{h}}$	$[\underline{\mathbf{y}}]_\alpha, \tilde{\mathbf{h}}$	$[\overline{\mathbf{y}}]_\alpha, \tilde{\mathbf{h}}$
0	-9.04873×10^{-5}	-4.87830×10^{-5}	0.81737	0.83220
0.5	-6.94694×10^{-5}	-4.97735×10^{-5}	0.82173	0.82913
1	-6.81546×10^{-5}	-6.35808×10^{-5}	0.82565	0.82564

Now, with the help of Equation (14) and the above formula, we have

$$\begin{cases} \mathscr{R}_k\left(\overrightarrow{\tilde{y}_{k-1}}(x;\alpha)\right) = \tilde{y}_{k-1}^{(\rho)}(x;\alpha) - \eta, \\ \left(\displaystyle\sum_{i=0}^{k-1}\tilde{y}_{k-1-i}(x;\alpha)\sum_{j=0}^{i}\tilde{y}_{i-j}(x;\alpha)\sum_{s=0}^{j}\tilde{y}_s(x;\alpha)\tilde{y}_{j-s}(x;\alpha)\right). \end{cases} \tag{40}$$

For the initial guess, we can choose

$$\tilde{y}_0(x;\alpha) = [1 + (-0.1 + 0.1\alpha)x,\ 1 + (0.1 - 0.1\alpha)x]. \tag{41}$$

For $k = 1$, we have

$$\tilde{y}_1(x;\alpha) = [1 - (0.1 - 0.1\alpha)x,\ 1 + (0.1 - 0.1\alpha)x] + \tilde{h}(\alpha)\tilde{y}_0(x;\alpha) - \eta\tilde{h}(\alpha)\tilde{\mathscr{J}}^{(\rho)}\left([\tilde{y}_0(x;\alpha)]^4\right). \tag{42}$$

For $k > 1$, we have

$$\begin{cases} \tilde{y}_k(x;\alpha) = [1 - (0.1 - 0.1\alpha)x,\ 1 + (0.1 - 0.1\alpha)x] \\ +(\tilde{y}_{k-1}(x;\alpha) - [1 - (0.1 - 0.1\alpha)x,\ 1 + (0.1 - 0.1\alpha)x]) \\ +\tilde{h}(\alpha)\tilde{y}_{k-1}(x;\alpha) - \eta\tilde{h}(\alpha)\tilde{\mathscr{J}}^{(\rho)}\left(\displaystyle\sum_{i=0}^{k-1}\tilde{y}_{k-1-i}(x;\alpha)\sum_{j=0}^{i}\tilde{y}_{i-j}(x;\alpha)\sum_{s=0}^{j}\tilde{y}_s(x;\alpha)\tilde{y}_{j-s}(x;\alpha)\right). \end{cases} \tag{43}$$

With the tenth-order FF-HAM approximate series solution $\tilde{y}(x;\tilde{h};\alpha) = \sum_{j=0}^{10}\tilde{y}_j(x,\tilde{h};\alpha)$. Since this equation is without an exact analytical solution, we can show the accuracy of the FF-HAM for Equation (36) by taking the residual error, as mentioned in Section 4, such that for $\eta = 0.6$, we have

$$\widetilde{\mathrm{ER}}(x;\alpha;\tilde{h}) = \tilde{y}^{(\rho)}(x;\alpha;\tilde{h}) - 0.6[\tilde{y}(x;\alpha;\tilde{h})]^4. \tag{44}$$

It is to be noted that series (44) depends upon x, α and the convergent control-parameter $\tilde{h}$. Toward this end, we have plotted the $\tilde{h}$-curve for $\tilde{y}(0.1;0.1;\tilde{h})$ via the tenth-order approximation of the FF-HAM. As in previous examples, we plotted the $\tilde{h}$-curve when $\alpha = 0.1$ to obtain the optimal value of $\tilde{h}$, as summarized in Figure 8.

According to Figure 8, from these curves, it is easy to discover the valid region of $\tilde{h}$ when the series solution of FF-HAM corresponds to the line segment that is nearly parallel to the horizontal axis such that the valid region of $\tilde{h}$ is bounded by $-0.7 \le \tilde{h} \le -0.1$. According to Section 4, the best values of $\tilde{h}$ can be obtained in that interval is $\tilde{h} = [-0.45259559205862615 - 0.42754247593277295]$. In the next table, we have tabulated the residual errors $[\underline{\mathrm{ER}}]_\alpha$ and $[\overline{\mathrm{ER}}]_\alpha$ of Equation (36) of the approximate solutions $\underline{y}(0.1;0.1;\tilde{h})$ and $\overline{y}(0.1;0.1;\tilde{h})$ obtained by using the tenth-order FF-HAM.

We can also summarize the solutions via the tenth-order FF-HAM for all $x \in [0, 0.1]$ and $\alpha \in [0, 1]$ corresponding with the best optimal convergence control values $\tilde{h}$ of Equation (36) in the following three-dimensional Figure 9.

Table 3 and Figure 9 illustrate the fuzzy solution of the temperature distribution equation. On the other hand, the proposed method solves the triangular solution of the fuzzy differential equation (28) with good accuracy for physical problems with strong nonlinearity.

6. Conclusion and Future Work

In this manuscript, the authors present a new convenient approximate analytical approach called the FF-HAM to solve linear and nonlinear FFBVP applications as physical problems. The concept of fuzzy set theory is discussed in conjunction with Caputo's fractional derivative characteristics for a novel FF-HAM form as well as a convergence algorithm. The numerical outputs proved that the proposed method is easy to implement and achieves the properties of the fuzzy set theory for FFBVPs in the form of triangular fuzzy numbers. Our approach has the advantage of giving more accurate outputs than other methods, such as the M6 method, and detecting the accuracy without requiring an exact solution, as with the temperature distribution equation. If you want to get closer to solving physical problems, it is proven that you should increase the number of FF-HAM series you make. The method can expand to solve fuzzy fractional chaotic systems and nonlinear partial differential equations which will be studied in future research work.

Data Availability

No data were used to support this study.

Conflicts of Interest

The authors declare that they have no conflicts of interest.

References

[1] C. Li and F. Zeng, "The finite difference methods for fractional ordinary differential equations," *Numerical Functional Analysis and Optimization*, vol. 34, no. 2, pp. 149–179, 2013.

[2] H. Beyer and S. Kempfle, "Definition of physically consistent damping laws with fractional derivatives," *ZAMM:Journal of Applied Mathematics and Mechanics*, vol. 75, no. 8, pp. 623–635, 1995.

[3] J. H. He, "Approximate analytical solution for seepage flow with fractional derivatives in porous media," *Computer Methods in Applied Mechanics and Engineering*, vol. 167, no. 1–2, pp. 57–68, 1998.

[4] S. S. Ray, A. Atangana, S. C. O. Noutchie, M. Kurulay, N. Bildik, and A. Kilicman, "Fractional calculus and its applications in applied mathematics and other sciences," *Mathematical Problems in Engineering*, vol. 2014, Article ID 849395, 2 pages, 2014.

[5] O. Abu Arqub, "Application of residual power series method for the solution of time-fractional Schrödinger equations in one-dimensional space," *Fundamenta Informaticae*, vol. 166, no. 2, pp. 87–110, 2019.

[6] S. Rekhviashvili, A. Pskhu, P. Agarwal, and S. Jain, "Application of the fractional oscillator model to describe damped vibrations," *Turkish Journal of Physics*, vol. 43, no. 3, pp. 236–242, 2019.

[7] K. M. Saad, E. H. F. Al-Shareef, A. K. Alomari, D. Baleanu, and J. F. Gómez-Aguilar, "On exact solutions for time-fractional Korteweg-de Vries and Korteweg-de Vries-Burger's equations using homotopy analysis transform method," *Chinese Journal of Physics*, vol. 63, pp. 149–162, 2020.

[8] M. A. Matlob and Y. Jamali, "The concepts and applications of fractional order differential calculus in modeling of viscoelastic systems: a primer," *Critical Reviews in Biomedical Engineering*, vol. 47, no. 4, pp. 249–276, 2019.

[9] M. Esmaeilbeigi, M. Paripour, and G. Garmanjani, "Approximate solution of the fuzzy fractional Bagley-Torvik equation by the RBF collocation method," *Comput. Methods Differ. Equations*, vol. 6, no. 2, pp. 186–214, 2018.

[10] A. F. Jameel, N. R. Anakira, A. K. Alomari, D. M. Alsharo, and A. Saaban, "New semi-analytical method for solving two point nth order fuzzy boundary value problem," *International Journal of Mathematical Modelling and Numerical Optimisation*, vol. 9, no. 1, pp. 12–31, 2019.

[11] M. Mosleh and M. Otadi, "Approximate solution of fuzzy differential equations under generalized differentiability," *Applied Mathematical Modelling*, vol. 39, no. 10–11, pp. 3003–3015, 2015.

[12] S. Hasan, A. Alawneh, M. Al-Momani, and S. Momani, "Second order fuzzy fractional differential equations under Caputo's H-differentiability," *Applied mathematics & information sciences*, vol. 11, no. 6, pp. 1597–1608, 2017.

[13] S. Askari, T. Allahviranloo, and S. Abbasbandy, "Solving fuzzy fractional differential equations by adomian decomposition method used in optimal control theory," *Mathamatics*, vol. 10, no. 12, pp. 1–10, 2019.

[14] E. Khodadadi and E. Çelik, "The variational iteration method for fuzzy fractional differential equations with uncertainty," *Fixed point theory and applications*, vol. 2013, no. 1, pp. 13–17, 2013.

[15] N. A. Khan, F. Riaz, and O. A. Razzaq, "A comparison between numerical methods for solving fuzzy fractional differential equations," *Nonlinear Engineering*, vol. 3, no. 3, pp. 155–162, 2014.

[16] E. Khodadadi, M. Karabacak, and E. Çelik, "Solving fuzzy fractional Riccati differential equations by the variational iteration method," *International Journal of Engineering and Applied Sciences*, vol. 2, no. 11, pp. 35–40, 2015.

[17] S. Liao, "On the homotopy analysis method for nonlinear problems," *Applied Mathematics and Computation*, vol. 147, no. 2, pp. 499–513, 2004.

[18] B. Ghazanfari and F. Veisi, "Homotopy analysis method for the fractional nonlinear equations," *Journal of King Saud University Science*, vol. 23, no. 4, pp. 389–393, 2011.

[19] Y. Tan and S. Abbasbandy, "Homotopy analysis method for quadratic Riccati differential equation," *Communications in Nonlinear Science and Numerical Simulation*, vol. 13, no. 3, pp. 539–546, 2008.

[20] M. M. Rashidi, G. Domairry, and S. Dinarvand, "Approximate solutions for the burger and regularized long wave equations by means of the homotopy analysis method," *Communications in Nonlinear Science and Numerical Simulation*, vol. 14, no. 3, pp. 708–717, 2009.

[21] S. Abbasbandy and M. Jalili, "Determination of optimal convergence-control parameter value in homotopy analysis method," *Numerical Algorithms*, vol. 64, no. 4, pp. 593–605, 2013.

[22] S. Bodjanova, "Median alpha-levels of a fuzzy number," *Fuzzy Sets and Systems*, vol. 157, no. 7, pp. 879–891, 2006.

[23] T. Allahviranloo, S. Salahshour, and S. Abbasbandy, "Explicit solutions of fractional differential equations with uncertainty," *Soft Computing*, vol. 16, no. 2, pp. 297–302, 2012.

[24] M. T. Mizukoshi, L. C. Barros, Y. Chalco-Cano, H. Román-Flores, and R. C. Bassanezi, "Fuzzy differential equations and the extension principle," *Information Sciences*, vol. 177, no. 17, pp. 3627–3635, 2007.

[25] S. Salahshour, T. Allahviranloo, and S. Abbasbandy, “Solving fuzzy fractional differential equations by fuzzy Laplace transforms,” *Communications in Nonlinear Science and Numerical Simulation*, vol. 17, no. 3, pp. 1372–1381, 2012.

[26] A. K. Alomari, M. I. Syam, N. R. Anakira, and A. F. Jameel, “Homotopy Sumudu transform method for solving applications in physics,” *Results in Physics*, vol. 18, pp. 103265–103274, 2020.

[27] D. J. Hashim, A. F. Jameel, T. Y. Ying, A. K. Alomari, and N. R. Anakira, “Optimal homotopy asymptotic method for solving several models of first order fuzzy fractional IVPs,” *Alexandria Engineering Journal*, vol. 61, no. 6, pp. 4931–4943, 2022, þ.

[28] I. Hashim, O. Abdulaziz, and S. Momani, “Homotopy analysis method for fractional IVPs,” *Communications in Nonlinear Science and Numerical Simulation*, vol. 14, no. 3, pp. 674–684, 2009.

[29] S. J. Liao, “An explicit, totally analytic approximate solution for blasius’ viscous flow problems,” *International Journal of Non-linear Mechanics*, vol. 34, no. 4, pp. 759–778, 1999.

[30] A. F. Jameel, N. R. Anakira, A. K. Alomari, M. A. Mahameed, and A. Saaban, “A new approximate solution of the fuzzy delay differential equations,” *International Journal of Mathematical Modelling and Numerical Optimisation*, vol. 9, no. 3, pp. 221–240, 2019.

[31] M. Ismail, U. Saeed, J. Alzabut, and M. ur Rehman, “Approximate solutions for fractional boundary value problems via green-CAS wavelet method,” *Mathematics*, vol. 7, no. 12, pp. 1164–1220, 2019.